

Iranian Journal of Oil & Gas Science and Technology, Vol. 10 (2021), No. 4, pp. 01–13
<http://ijogst.put.ac.ir>

Predicting the Permeability Using Geometric Properties of Micro-Computed Tomography Images by Linear Regression Models

Mohammad Ashrafi¹, Seyyed Alireza Tabatabaei-Nejad^{2*}, and Elnaz Khodapanah³

¹ Ph.D. Candidate, Department of Petroleum and Natural Gas Engineering, Sahand Oil and Gas Research Institute (SOGRI), Sahand University of Technology, Tabriz, Iran

² Professor, Department of Petroleum and Natural Gas Engineering, Sahand Oil and Gas Research Institute (SOGRI), Sahand University of Technology, Tabriz, Iran

³ Associate Professor, Department of Petroleum and Natural Gas Engineering, Sahand Oil and Gas Research Institute (SOGRI), Sahand University of Technology, Tabriz, Iran

Highlights

- Minkowski functional calculation is employed for 20 series of micro-computed tomography images;
- A linear regression model to predict absolute permeability is proposed;
- An extensive study is conducted on the geometric properties of rock images.


Received: June 02, 2021; *revised:* July 19, 2021; *accepted:* July 07, 2021

Abstract

Challenges of rock absolute permeability prediction of tiny samples are remarkable when laboratory apparatus is not applicable and there is no pore network modeling. The prediction using the characterization of micro-computed tomography images has been studied in this paper. Twenty series of 2D micro-computed tomography rock binary images have been collected, and each was considered a 3D binary image. Their geometric measures in 2D and 3D for measuring image properties have been considered using Minkowski functionals and available functions, developing a regression model; absolute permeabilities have also been evaluated. Some 2D and 3D geometric properties are considered. The area, the perimeter, and the 2D Euler number are 2D binary image properties. The volume, surface area, mean breadth, integral of the mean curvature, and the 3D Euler number are 3D binary image properties. The porosity and number of objects have also been considered parameters of a regression model. Twenty-four parameters were evaluated, and some were chosen to perform linear regression. An equation was proposed based on the extensive study to predict rock permeability. This equation has two sets of parameter coefficients: one set predicts high-permeability rocks (above two Darcy), and the other used for low- and medium-permeability rocks (less than two Darcy) can be employed for carbonated rock. The average absolute relative error for conducted cases is 0.06.

Keywords: Absolute Permeability; Euler Number; Minkowski Functions; 2D Binary Image; 3D Image

How to cite this article

Ashrafi M, Tabatabaei-Nejad S.A.R, Khodapanah E, Predicting the Permeability Using Geometric Properties of Micro-Computed Tomography Images by Linear Regression Models, Iran J. Oil Gas Sci. Technol., Vol. 10, No. 4, pp. 01–13, 2021. DOI: <http://dx.doi.org/10.22050/ijogst.2021.289006.1597> This is an Open Access article under Creative Commons Attribution 4.0 International License. (creativecommons.org/licenses/by/4.0) 

* Corresponding author :

Email: tabatabaei@sut.ac.ir

1. Introduction

Absolute permeability is an essential macroscopic property of porous media depending on its microscopic properties. Topological and geometrical properties and their relation with macroscopic properties such as permeability, porosity, and formation factor are greatly interesting for researchers. Nowadays, different techniques have been developed to characterize porous media (Gao et al., 2019; Hu et al., 2017).

Among these methods, micro-computed tomography, known as micro-CT imaging, is the most referred technique (Bartels et al., 2019). Permeability prediction from the direct application of Navier–Stokes equation on pore network has the problem of method selection, and convergence may occur. In other words, if one can find the relationship between some image properties with desired permeability, then the prediction of the desired property will be simple.

Estimating permeability using rock properties was started by the Kozeny–Carman equation and developed in recent years when some parameters such as porosity or tortuosity were included (Berg, 2014; Dabek et al., 2014). Benavente et al. (2015) proposed permeability prediction in sandstones and carbonated rock through a series of statistical models based on capillary imbibition, porosity, and pore structure.

Standard parameters used in the quantitative analysis of spatial structures are area, perimeter in 2D, volume, surface area, and the mean breadth in 3D. Another parameter is the Euler–Poincaré characteristic, related to the topology of the structure. These parameters form the so-called Minkowski functionals that encompass standard geometric parameters such as volume, area, length, and the Euler–Poincaré characteristic. The Euler–Poincaré characteristic is a standard connectivity parameter and equals the number of the connected components minus its number of holes for a planar structure. Using Euler characteristic and void ratio, Liu and coworkers predicted permeability in 3D porous media (Liu et al., 2017). Botha and coworker calculated the coefficient of determination from ordinary least squares modeling calculated characteristic (from the 5, 16, and 64 mm/voxel images) with lattice Boltzmann permeability from the 5 mm/voxel image (Botha and Sheppard, 2016). Their calculated characteristic consists of rock fabric, pore system, and Minkowski functionals. Saxena et al. concluded that reasonably accurate estimates of the permeability of natural rocks could be obtained from 2D thin sections without the reconstruction of the 3D rock, especially for sandstones (Saxena et al., 2017; Rabbani and Ayatollahi, 2015). Scholz et al. studied the relationship between permeability and morphology for porous structures composed of randomly placed overlapping circular or elliptical grains. They generalized arbitrary structures modeled and characterized by Minkowski functionals (Scholz et al., 2015). Based on the performed study herein, the idea to predict permeability from a series of 2D images of rock is investigated, and two regression models have been developed.

2. Methods

Methods predicting permeability are going to be investigated herein. The study conducted herein is based on a statistical method to find a correlation to predict permeability using 2D and 3D image properties. In the following, parameters are going to be described.

The area of an object and NumObjects are based on MATLAB documentation; the area of an object in the binary image corresponds roughly to the total number of pixels in the image but may not be the same because various patterns of pixels are weighted differently. An algorithm estimates the area of all of the pixels in an image by summing the areas of each pixel in the image. The area of an individual pixel is determined by looking at its 2-by-2 neighborhood. There are six different patterns, each representing a different area. Patterns with zero on pixels, one on pixels, two adjacent on pixels, two

diagonals on pixels, three on pixels, and all four on pixels are proportional to the area of 0, 1/4, 1/2, 3/4, 7/8, and 1.0. In the algorithm, each pixel is part of four different 2-by-2 neighborhoods, indicating that a single on a pixel surrounded by off pixels has a total area of 1.0. NumObjects is the number of connected components (objects) in a binary image: connectivity of 4 and 8 for two dimensions; 6, 18, and 26 for three dimensions can be considered (MATLAB and Statistics Toolbox Release, 2012b).

The Euler number for the 2D binary image is a scalar whose value is the total number of objects in the image minus the total number of holes in those objects. Four-connected objects and eight-connected objects can be considered. If it is nonzero, a pixel is a part of the perimeter and connected to at least one zero-valued pixel. The connectivity can be 4 or 8 for two dimensions, 6, 18, or 26 for three dimensions (Legland et al., 2007).

Minkowski geometric measures for 2D image parameters are the area, the perimeter, and the (2D) Euler number; for 3D images, the parameters are the volume, the surface area (called surface), the mean breadth (also known as the integral of the mean curvature) and the (3D) Euler number. An algorithm given by Legland called imMinkowski can help calculate some of Minkowski's properties (Legland et al., 2007).

3. Results and discussion

Twenty series of 2D micro-CT images of Imperial Colleague as listed in Table 1 have been studied. Among these series, six of them are sand packs named FA, FB, FC, LVA, LVB, and LVC; A1 is synthetic silica, and C1 and C2 are carbonated; Est is limestone, and S1, S2, S3, S4, S5, S6, S7, S8, S9 and Berea are sandstones (Dong, 2008; Muljadi et al., 2016).

Table 1
The size and resolution of the 20 series of micro-CT images (Dong, 2008; Muljadi et al., 2016).

Sample ID	Size	Resolution (micron/voxel)	Sample ID	Size	Resolution (micron/voxel)
S1	300 × 300 × 300	8.643	C1	400 × 400 × 400	2.85
S2	300 × 300 × 300	4.956	C2	400 × 400 × 400	5.345
S3	300 × 300 × 300	9.10	FA	450 × 450 × 450	9.996
S4	300 × 300 × 300	8.96	FB	450 × 450 × 450	10.002
S5	300 × 300 × 300	3.997	FC	450 × 450 × 450	10.002
S6	300 × 300 × 300	5.10	Berea	400 × 400 × 400	5.345
S7	300 × 300 × 300	4.803	LA	450 × 450 × 450	10.002
S8	300 × 300 × 300	4.892	LB	450 × 450 × 425	8.851
S9	300 × 300 × 300	3.398	LC	450 × 450 × 450	10.002
A1	300 × 300 × 300	3.85	Est	650 × 650 × 650	3.3113

One slice of some series of the images is depicted in Figure 1, and a list of different properties and their definitions used in our study are listed in Table 2.

Table 2
Parameters definition and their correlation coefficient versus reported permeability.

Parameter	Definition	Method of calculation	R vs. reported permeability
Porosity	Porosity	MATLAB function	0.651
A2	The 2D area	imMinkowski	-0.309
P22	The 2D perimeter of 2 connectivity	imMinkowski	0.143
P24	The 2D perimeter of 4 connectivity	imMinkowski	0.137
E24	The 2D Euler number of 4 connectivity	imMinkowski	-0.495
E28	The 2D Euler number of 8 connectivity	imMinkowski	0.558
bw2p4	The 2D perimeter of 4 connectivity	MATLAB function	-0.423
bw2p8	The 2D perimeter of 8 connectivity	MATLAB function	-0.418
NObw2c4	The 2D number of objects of 4 connectivity	MATLAB function	-0.405
NObw2c8	The 2D number of objects of 8 connectivity	MATLAB function	-0.457
bw2a	The 2D area	MATLAB function	-0.517
V3	The 3D Volume	imMinkowski	-0.309
S33	The 3D surface of 3 paths	imMinkowski	0.045
S313	The 3D surface of 13 paths	imMinkowski	0.028
B33	The 3D mean breadth of 3 path	imMinkowski	-0.511
B313	The 3D mean breadth of 13 path	imMinkowski	-0.506
E36	The 3D Euler number of 6 connectivity	imMinkowski	0.603
E326	The 3D Euler number of 26 connectivity	imMinkowski	0.298
NObw3c6	The 3D number of objects of 6 connectivity	MATLAB function	-0.096
NObw3c18	The 3D number of objects of 18 connectivity	MATLAB function	-0.319
NObw3c26	The 3D number of objects of 26 connectivity	MATLAB function	-0.333
bw3p6	The 3D perimeter of 6 connectivity	MATLAB function	-0.277
bw3p18	The 3D perimeter of 18 connectivity	MATLAB function	-0.385
bw3p26	The 3D perimeter of 26 connectivity	MATLAB function	-0.393

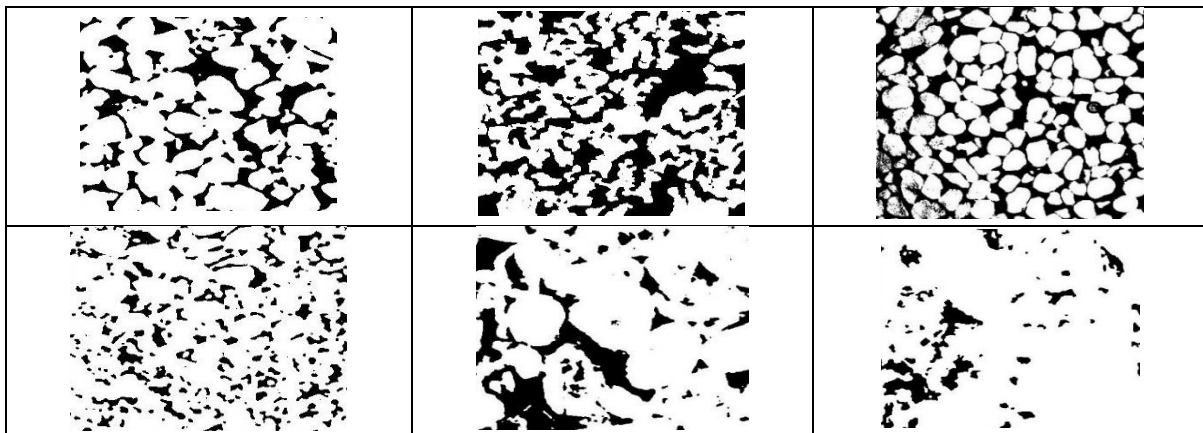


Figure 1

The 2D binary image of some cases: from left to right and up to down the image belongs to S2, A1, LA, S3, and C1 (Dong, 2008; Muljadi et al., 2016).

Two functions are used to obtain properties: one is from the library functions of MATLAB, and the other is the algorithm written by Legland et al. (2007). The 24 parameters are calculated for 20 available cases. The correlation coefficient of each parameter versus its reported permeability is also obtained; parameter definition and calculation method are listed in Table 2, and the results are presented in Tables 3–6. The correlation coefficient (R) is calculated by Equation (1).

$$R = \frac{\sum_m \sum_n (A_{mn} - \bar{A})(B_{mn} - \bar{B})}{\sqrt{(\sum_m \sum_n (A_{mn} - \bar{A})^2)(\sum_m \sum_n (B_{mn} - \bar{B})^2)}} \quad (1)$$

where R is the correlation coefficient, \bar{A} indicates the average of A , and \bar{B} represents the average of B . To calculate the correlation coefficient of the parameter versus permeability, A is the reported permeability, B is the value of the parameter, n equals 1, and m is equal to 20 as 20 cases are studied.

The correlation coefficient of every two of the parameters is calculated to investigate the relationship between all the parameters. When the correlation coefficient between two parameters is 1.0, using the two parameters gives the same results. Based on the conducted study, the correlation coefficient between A2 and V3 is 1.0. A correlation coefficient between two investigating parameters approaching 1.0 or being greater than 0.9 shows no privilege of selecting between any of these two parameters. The correlation coefficient between bw2p4 and bw2p8, B33 and B313, P22 and P24, S33 and S313, E24 and E28, and NObw2c4 and NObw2c8 is 0.99. The correlation coefficient between P22 and S33 and between NObw2c4 and E24 is also 0.98. Further, the correlation coefficient between any two parameters of NObw3c18, NObw3c26, bw3p6, bw3p18, bw3p26 is higher than 0.90.

Table 3
Parameters values of S1, S2, S3, S4, and S5.

Parameter	S1	S2	S3	S4	S5
Porosity	0.141	0.246	0.169	0.171	0.211
A2	1.002147	1.001126	0.997458	1.001506	1.001465
P22	90.20332	83.0798	147.4799	148.3414	49.34178
P24	90.469	83.14083	147.1579	148.163	49.7437
E24	0.000718	0.000694	0.002575	0.002775	0.00025
E28	0.000716	0.000664	0.0025	0.002715	0.000238
bw2p4	9.092578	14.75976	13.51054	13.78178	11.11281
bw2p8	12.43035	20.35053	18.03157	18.36116	15.18527
NObw2c4	0.000731	0.000736	0.002603	0.002817	0.000285
NObw2c8	0.000729	0.00071	0.002534	0.002763	0.000275
bw2a	0.013583	0.041255	0.012279	0.012714	0.063128
V3	1.002147	1.001126	0.997458	1.001506	1.001465
S33	127.1385	113.9553	216.2687	217.0337	67.31697
S313	129.0639	114.5961	216.9746	217.9871	68.23403
B33	559.3144	317.439	1799.836	1871.176	128.8573
B313	575.1237	324.724	1809.792	1885.001	132.1661
E36	-2.03E-05	-8.44E-05	-0.00011	2.33E-06	-6.70E-06
E326	-3.90E-05	-0.0001	-0.00023	-0.00011	-1.48E-05

Parameter	S1	S2	S3	S4	S5
NObw3c6	1.76E-05	2.92E-05	0.000139	0.00015	1.76E-05
NObw3c18	1.47E-05	1.86E-05	9.24E-05	0.00011	1.34E-05
NObw3c26	1.43E-05	1.71E-05	8.47E-05	0.000103	1.28E-05
bw3p6	0.000125	0.000119	0.000823	0.000875	8.36E-05
bw3p18	0.000104	7.57E-05	0.000547	0.000643	6.35E-05
bw3p26	0.000101	6.97E-05	0.000501	0.000602	6.07E-05
Reported K (mD)	1969	4318	143	273	4638

Table 4
Parameters values of S6, S7, S8, S9, and Berea.

Parameter	S6	S7	S8	S9	Berea
Porosity	0.24	0.251	0.34	0.222	0.196
A2	0.998304	0.997936	0.999446	0.998855	1.002311
P22	46.44874	63.75716	61.48692	52.07811	138.0109
P24	46.86053	63.86119	61.95136	52.5002	137.0187
E24	0.000187	0.000353	0.000259	0.000356	0.001121
E28	0.000163	0.000334	0.000252	0.000352	0.001064
bw2p4	8.250154	11.80653	11.3862	13.73165	22.01797
bw2p8	11.26511	16.34587	15.6979	18.77376	30.22633
NObw2c4	0.000272	0.000407	0.00039	0.000373	0.0012
NObw2c8	0.000258	0.000393	0.000386	0.000369	0.001151
bw2a	0.03864	0.04367	0.042139	0.087147	0.035618
V3	0.998304	0.997936	0.999446	0.998855	1.002311
S33	64.1063	87.29302	87.36279	66.89002	177.8504
S313	65.25598	88.12214	89.0066	67.94605	175.6787
B33	75.61574	150.6109	114.683	145.5255	978.75
B313	79.28986	155.7216	124.0396	149.5879	977.0689
E36	-2.36E-05	-5.59E-05	-6.06E-05	-1.04E-05	-6.83E-05
E326	-1.94E-05	-6.01E-05	-7.82E-05	-1.60E-05	-8.54E-05
NObw3c6	1.66E-05	1.40E-05	4.36E-05	4.85E-06	4.28E-05
NObw3c18	1.12E-05	9.19E-06	3.80E-05	4.44E-06	3.65E-05
NObw3c26	1.02E-05	8.22E-06	3.66E-05	4.37E-06	3.52E-05
bw3p6	6.91E-05	5.56E-05	0.000128	2.19E-05	0.000219
bw3p18	4.66E-05	3.66E-05	0.000112	2.00E-05	0.000186
bw3p26	4.24E-05	3.28E-05	0.000108	1.97E-05	0.000179
Reported K (mD)	11289	7268	13063	2735	1360

Table 5
Parameters values of sand packs.

Parameter	LA	LB	LC	FA	FB	FC
Porosity	0.377	0.368	0.372	0.33	0.333	0.331
A2	0.963074	1.002045	0.990353	0.97602	0.998468	0.993435
P22	138.2828	129.3873	149.155	108.7522	110.3502	110.735
P24	138.2299	128.7611	148.5314	108.0377	110.0948	110.8092
E24	-0.00012	-0.00012	-4.48E-05	0.000417	-1.00E-05	-3.95E-05
E28	-0.00027	-0.00026	-0.00023	6.91E-06	-7.29E-05	-8.19E-05
bw2p4	12.36288	12.98506	13.22793	9.5262	9.825293	9.943895
bw2p8	16.83466	17.86725	18.07862	12.98176	13.52377	13.72843
NObw2c4	0.000366	0.000319	0.000438	0.000673	0.000205	0.000174
NObw2c8	0.000292	0.00025	0.000343	0.000378	0.000168	0.000151
bw2a	0.009772	0.012968	0.010058	0.009883	0.010097	0.010045
V3	0.963074	1.002045	0.990353	0.97602	0.998468	0.993435
S33	182.4199	161.8595	194.2795	138.8215	142.5115	143.5906
S313	181.2389	160.4597	192.2729	137.212	141.999	143.645
B33	46.81403	-4.67593	88.44484	271.1291	68.0258	41.72094
B313	80.34152	21.58291	120.0397	262.9103	95.92433	63.78165
E36	-0.00064	-0.0005	-0.0007	-0.00028	-0.00029	-0.0002
E326	-0.00033	-0.00025	-0.00038	-0.0001	-9.72E-05	-9.52E-05
NObw3c6	3.38E-05	3.08E-05	3.86E-05	0.000138	2.15E-05	1.73E-05
NObw3c18	1.83E-05	1.70E-05	1.98E-05	3.98E-05	1.16E-05	8.90E-06
NObw3c26	1.59E-05	1.50E-05	1.72E-05	2.96E-05	9.96E-06	7.55E-06
bw3p6	8.97E-05	8.36E-05	0.000104	0.000418	6.46E-05	5.22E-05
bw3p18	4.85E-05	4.61E-05	5.33E-05	0.000121	3.49E-05	2.69E-05
bw3p26	4.22E-05	4.07E-05	4.61E-05	8.97E-05	2.99E-05	2.28E-05
Reported K (mD)	35300	31500	19400	59000	52300	50400

Table 6
Parameter values of A1, C1, C2, and Est.

Parameter	A1	C1	C2	Est
Porosity	0.429	0.23	0.168	0.108
A2	0.99919	1.011364	1.001831	1.197512
P22	71.94223	83.32853	122.5244	152.9284
P24	73.99697	83.52677	122.299	154.9405
E24	0.000954	0.000539	0.00111	0.00025
E28	0.000812	0.000488	0.001051	0.000246
bw2p4	17.33644	25.78892	19.58634	41.74955
bw2p8	22.44355	35.14716	26.52617	56.58973
NObw2c4	0.001012	0.000684	0.001225	0.000287

Parameter	A1	C1	C2	Est
NObw2c8	0.000874	0.00065	0.001181	0.000284
bw2a	0.068026	0.125627	0.035515	0.110099
V3	0.99919	1.011364	1.001831	1.197512
S33	104.1238	122.6036	173.7738	199.4889
S313	107.8335	123.6523	173.9117	204.2984
B33	206.9308	546.9094	1366.24	1021.263
B313	195.5594	546.3308	1360.511	1059.566
E36	-5.89E-05	2.38E-06	3.49E-05	-1.73E-05
E326	-0.00023	-2.13E-05	-1.95E-05	-1.89E-05
NObw3c6	0.000184	8.99E-05	0.00015	1.95E-06
NObw3c18	3.32E-05	6.71E-05	0.00012	1.93E-06
NObw3c26	3.22E-06	6.34E-05	0.000114	1.92E-06
bw3p6	0.00043	0.000391	0.000893	1.81E-05
bw3p18	7.74E-05	0.000292	0.000712	1.79E-05
bw3p26	7.51E-06	0.000276	0.000678	1.78E-05
Reported K (mD)	8272	785	38	172

Based on the generated data and used parameters, a linear regression model to predict a variety of absolute permeabilities of rock was developed. The linear model was selected because it is simple and easy to work. The number of the parameters used in the equation was a challenge. Finally, after creating a linear model with different parameters, the model with the least number of parameters that can better predict the reported data was selected. Among parameters listed in Table 2, there are some parameter groups the members of which have the same behavior, so only one parameter from each group is considered in the final model expressed in Equation (2).

Two sets of coefficient parameters were generated as listed in Table 7 to cover the full range of permeabilities. One set of coefficients was related to rocks with permeability lower than 2 Darcy, and the other set was related to those with permeability above 2 Darcy. In the case of permeability of 2 Darcy, both sets can be used.

$$\begin{aligned}
 K \text{ (mD)} = & a1 \times \text{porosity} + a2 \times \text{bw2a} + a3 \times A2 + a4 \times P22 + a5 \times \text{bw2p4} \\
 & + a6 \times B33 + a7 \times \text{NObw3c6} + a8 \times \text{NObw3c18} + a9 \times E36 \\
 & + a10 \times E326 + a11 \times E24
 \end{aligned} \quad (2)$$

where K is absolute permeability, bw2a indicates the 2D area calculated by MATLAB function, $a2$ is the 2D area calculated by imMinkowski , $P22$ stands for the 2D perimeter of objects of two connectivity, bw2p4 denotes the 2D perimeter of objects of four connectivity, $B33$ is the 3D mean breadth of three paths, NObw3c6 represents the 3D number of objects of six connectivity, NObw3c18 is the 3D number of objects of 18 connectivity, $E36$ represents the 3D Euler number of objects of six connectivity, $E326$ indicates the 3D Euler number of objects of 26 connectivity, and $E24$ stands for the 2D Euler number of objects of four connectivity.

Table 7
The parameter coefficients of Equation (2).

Parameter coefficient	$K < 2D$	$K > 2D$
a_1	2561.601898	166606.9314
a_2	0	204150.3261
a_3	-107.2069415	-37398.83022
a_4	50.22296765	798.0438519
a_5	-78.44146504	-3913.780701
a_6	-4.48472775	10.4925334
a_7	0	-107437068.7
a_8	0	-263709565.6
a_9	20298580.14	0
a_{10}	0	184072600.5
a_{11}	-15481223.59	0

Predicted permeabilities calculated by Equation (2) versus the reported permeabilities in Table 8 are shown in Figures 2 and 3. The proposed equation results can predict the absolute permeability of sandstone and carbonate rocks within a different range of permeabilities. The average absolute relative error is 0.06, showing that the equation can predict absolute permeability well.

Table 8
Reported permeabilities versus those calculated by Equations (2) and (3).

Sample ID	Reported K	Calculated K	Relative Error
S1	1969	1968.99	0.00
S2	4318	3657.08	0.15
S3	143	142.99	0.00
S4	273	272.99	0.00
S5	4638	3456.79	0.25
S6	11289	11369.76	-0.01
S7	7268	7682.94	-0.06
S8	13063	13849.23	-0.06
S9	2735	3171.73	-0.16
A1	8272	8403.18	-0.02
C1	785	784.99	0.00
C2	38	37.99	0.00
FA	59000	58769.71	0.00
FB	52300	51882.9	0.01
FC	50400	51923.13	-0.03
Berea	1360	1359.99	0.00
LA	35300	29310.79	0.17
LB	31500	31678.31	-0.01
LC	19400	24160.13	-0.25
Est	172	171.99	0.00
Average absolute relative error			0.06

Absolute permeability calculation from an approximately large sample compared to the small sample in the range of millimeters in laboratory is used wildly. When a small sample is available, pore network extraction with the help of proper modeling and application of the Naiver–Stock equation is a good solution; however, there are some problems during the network extraction process and assigning pores and throats to void spaces.

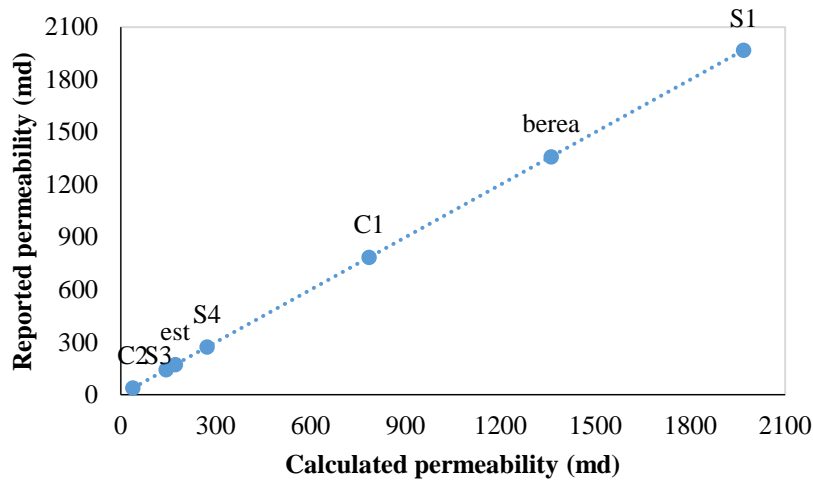


Figure 2

The prediction of permeability by Equation (2) when $K < 2D$ versus the reported permeability.

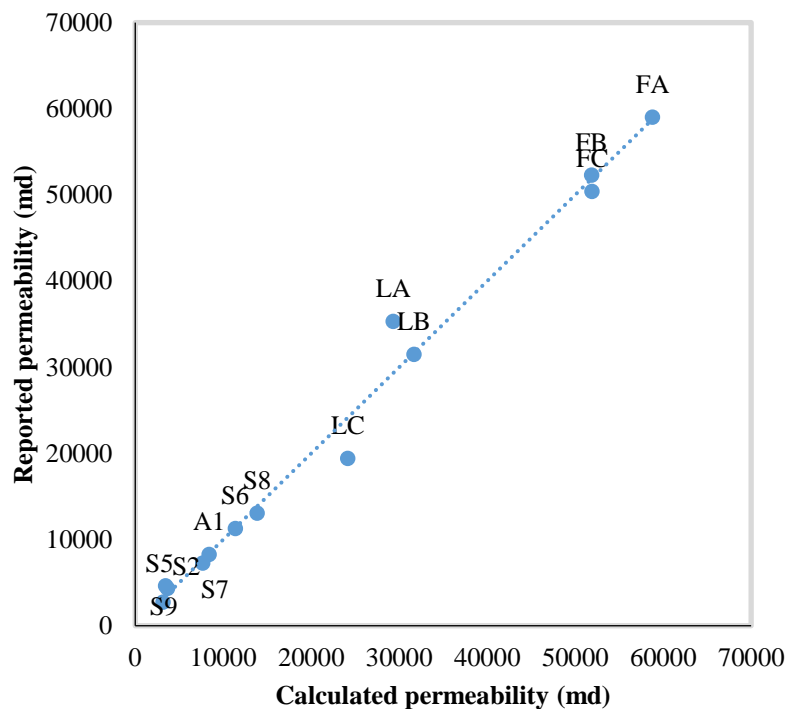


Figure 3

The prediction of permeability by Equation (2) when $K > 2D$ versus the reported permeability.

This study introduced an easy way to predict absolute permeability by considering geometric properties. An excellent study on finding statistical relationships between geometric properties derived from CT

scan results and permeability is presented. However, the applicability of the developed regression models to uncored intervals is not limited. When a large plug sample or core is not available and the subject only studies tiny rock cuttings, proper precise imaging and the proposed method can be a fast and accurate solution.

The method applicable to permeability calculation is not very expensive since it does not demand laboratory typical flooding and only routine CT scan analysis coupled by the equation can evaluate the absolute permeability. Researchers look for cost-effective methods to estimate permeability, and the introduced method is less expensive than the special core analysis (SCAL) tests such as air injection for permeability measurement of plugs. Moreover, the sample remains unchanged after the analysis.

It appears necessary to compare the result from this studied method with the laboratory results on a particular rock as a case study. The point is that the introduced method is applicable to tiny samples that can be imaged around 1 mm^3 , while the smallest plug must put on the core flooding apparatus is around 10 cm^3 . Considering the heterogeneity available in all porous media, the laboratory results of a large sample are not identical to the results from the tiny images. The new method can efficiently predict the permeability of even small drilling cuttings. The next advantage of the method compared to core flooding is that the sample remains clean and unchanged after imaging. The disadvantage of the method is that micro-CT imaging is expensive, and evaluating the parameter for large images needs a high-technology processor.

However, the data set used in this study was gathered by Dong (2008), which is a validated source for digital rock researchers. The reported permeability presented in Figures 2 and 3 is extracted from widely referred validated data of Dong's thesis (Dong, 2008) and compared with the calculated permeability. The average absolute relative error for the calculated values is 0.06, implying that the new model predicts permeability excellently.

4. Conclusions

Predicting absolute permeability as a petrophysical property was studied, and an equation was proposed using 20 series of micro-CT images. Different properties were selected to conduct this study. Among the selected properties, porosity and 3D Euler number of six connectivity have higher correlation coefficients when correlated by reported permeabilities. It was found that there was a strong relationship between some parameters such as P24 and P22, E24 and E28, bw2p4 and bw2p8, V3 and A2, B313 and B33, S313 and S33, and Nobw2c4 and Nobw2c8. Hence, using any pairs of parameters yields the same results. The proposed equation with two sets of parameter coefficients excellently predicts the absolute permeability using geometric properties. One set is appropriate for permeability values higher than 2 Darcy, and the other is for cases with a permeability value lower than 2 Darcy for different rock types. The equation is applied to 20 series with an average absolute relative error of 0.06.

When an enough large sample for laboratory core flooding apparatus is not available, imaging is a good solution. Further, the newly developed pore network extraction has severe problems regarding pore and throat assignment and a relatively high error during solving the applied model parameters; thus, the idea introduced herein is to consider geometric properties and evaluate linear regression models to predict absolute permeability easily and quickly. Maybe at the first look, the proposed equation has an overfitting problem; however, all the studied parameters are not added to the regression analysis as the correlation coefficient, and only essential parameters significantly affecting the permeability are considered.

Founding

This research did not receive any specific grant from funding agencies in the public, commercial, or not-for-profit sectors.

Nomenclature

A2	2D area
B313	The 3D mean breadth of 13 path
B33	The 3D mean breadth of 3 path
Bw2a	2D area
Bw2p4	The 2D perimeter of 4 connectivity
Bw2p8	The 2D perimeter of 8 connectivity
Bw3p6	The 3D perimeter of 6 connectivity
Bw3p18	The 3D perimeter of 18 connectivity
Bw3p26	The 3D perimeter of 26 connectivity
CT	Computed tomography
E24	The 2D Euler number of 4 connectivity
E28	The 2D Euler number of 8 connectivity
E36	The 3D Euler number of 6 connectivity
E326	The 3D Euler number of 26 connectivity
<i>K</i>	Absolute permeability
mm	Millimeter
NObw2c4	The 2D number of objects of 4 connectivity
NObw2c8	The 2D number of objects of 8 connectivity
NObw3c6	The 3D number of objects of 6 connectivity
NObw3c18	The 3D number of objects of 18 connectivity
NObw3c26	The 3D number of objects of 26 connectivity
P22	The 2D perimeter of 2 connectivity
P24	The 2D perimeter of 4 connectivity
S313	The 3D surface of 13 paths
S33	The 3D surface of 3 paths
SCAL	Special core analysis
V3	3D volume
<i>R</i>	Correlation coefficient
<i>R</i> ²	<i>R</i> -squared

References

- Bartels, W. B., Rücker, M., Boone, M., Bultreys, T., Mahani H., Berg, S., Imaging Spontaneous Imbibition in Full Darcy-scale Samples at Pore-scale Resolution by Fast X-Ray Tomography, *Water Resources Research*, Vol.55, p.7072– 7085, 2019. <https://doi.org/10.1029/2018WR024541>
- Benavente, D., Pla, C., Cueto, N., Galvan, S., Martinez-Martinez, J., Garcia-Del-Cura, M. A., Ordonez, S., Predicting Water Permeability in Sedimentary Rocks from Capillary Imbibition and Pore Structure, *Eng. Geol.*, Vol.195, p.301–311, 2015. <https://doi.org/10.1016/j.enggeo.2015.06.003>.

- Berg, C. F., Permeability Description by Characteristic Length, Tortuosity, Constriction and Porosity, *Transp. Porous Media*, Vol.103, No.3, p.381–400, 2014, <https://doi.org/10.1007/S11242-014-0307-6>.
- Botha, P. W. S. K., Sheppard, A. P., Mapping Permeability in Low-Resolution Micro-CT Images: A Multiscale Statistical Approach, *Water Resour. Res.*, Vol.52, p.4377–4398, 2016. <https://doi.org/10.1002/2015WR018454>.
- Dabek, L., Shad, S., Dalir A., Knepp, R., Correlation of Permeability and Volume of Shale in Oil Sands: Improving Predictability in Low Permeability Zones of The McMurray Formation, Alberta, Canada, SPE Heavy Oil Conference-Canada, 2014. <https://doi.org/10.2118/170060-MS>
- Dong, H., Micro-CT Imaging and Pore Network Extraction, Ph.D. Diss., Department of Earth Science and Engineering, Imperial College London, 2008.
- Gao, Z., Yang, X., Hu, C., Wei, L., Jiang, Z., Yang, S., Fan, Y., Xue, Z., Yu, H., Characterizing the Pore Structure of Low Permeability Eocene Liushagang Formation Reservoir Rocks from Beibuwan Basin in Northern South China Sea, *Mar. Petrol. Geol.* Vol.99, p.107–121, 2019. <https://doi.org/10.1016/J.MARPETGEO.2018.10.005>.
- Hu, Q., Zhang, Y., Meng, X., Li, Z., Xie, Z., Li, M., Characterization of Micro-Nano Pore Networks in Shale Oil Reservoirs of Paleogene Shahejie Formation in Dongying Sag of Bohai Bay Basin, East China, *Petrol. Explor. Dev.* Vol.44, p.720–730, 2017. [https://doi.org/10.1016/S1876-3804\(17\)30083-6](https://doi.org/10.1016/S1876-3804(17)30083-6).
- Legland, D., Kieu, K., Devaux, M., Computation Of Minkowski Measures on 2D and 3D Binary Images, *Image Analysis and Stereology*, Vol 26, No.2, 2007. <https://doi.org/10.5566/Ias.V26.P83-92>
- Liu, Z., Herring, A. L., Robins, V., Armstrong, R. T., Prediction of Permeability from Euler Characteristic of 3D Images, in *International Symposium of The Society of Core Analysts*, 2017.
- MATLAB and Statistics Toolbox Release 2012b, The MathWorks, Inc., Natick, Massachusetts, United States. <https://www.mathworks.com/help/images/index.html>
- Muljadi, B. P., Blunt, M. J., Raeini, A. Q., Bijeljic, B., The Impact of Porous Media Heterogeneity on Non-Darcy Flow Behavior from Pore-scale Simulation, *Advances in Water Resources*, Vol. 95, p. 329–340, 2016. <https://doi.org/10.1016/J.Advwatres.2015.05.019>
- Rabbani, A., Ayatollahi, S. H., Comparing Three Image Processing Algorithms to Estimate The Grain-Size Distribution of Porous Rocks from Binary 2D Images and Sensitivity Analysis of The Grain Overlapping Degree, *Special Topics and Reviews in Porous Media, An International Journal*, Vol.6, p.71–89, 2015. <https://doi.org/10.1615/Specialtopicsrevporousmedia.V6.I1.60>
- Saxena, N., Mavko, G., Hofmann, R., Srisutthiyakorn, N., 2017. Estimating Permeability from Thin Sections without Reconstruction: Digital Rock Study of 3D Properties from 2D Images, United Kingdom. <https://doi.org/10.1016/J.Cageo.2017.02.014>.
- Scholz, C., Wirner, F., Klatt, M., Hirneise, A., Schroder-Turk, G. E., Mecke, K., Bechinger, C., Direct Relations between Morphology and Transport in Boolean Models, *Physical Review E*; Vol. 92, 043023, 2015. <https://doi.org/10.1103/Physreve.92.043023>